

## 2. Data and Methods

### 2.1. SHIP MEASUREMENTS

CTD data were obtained during the international CoMSBlack and NATO TU Black Sea cruises during April 1993 and May 1994. Acquisition and processing of CTD data were described in the series of NATO TU Black Sea Project Technical reports. Detailed description of the data can be found in [5]. Current measurements were performed on board of R/V Bilim of the Institute of Marine Sciences Middle East Technical University, Turkey both at hydrographic stations and along the ship tracks using the hull mounted 150kHz ADCP (Acoustic Doppler Current Profiler) from RD Instruments while ship was cruising between stations. The measurements were made using an ensemble averaging period of 5 minutes at a rate of 60 pings per minute, a pulse length of 4 m, and a vertical bin length of 4 m. Ship gyro was used to convert the velocities measured relative to the ship coordinate to the earth referenced coordinate. Ship location at each ensemble were fixed using Global Positioning System (GPS). Relative velocities were converted to absolute velocities using bottom track where the ADCP was able to detect the bottom. This was usually possible in water depths less than about 400m. An analysis intended to calculate absolute water velocities by subtracting ship velocities calculated from GPS fixes from the Doppler velocity (water velocity relative to ship velocity). The GPS precision during April 1993 measurements was appropriate to present velocities from this cruise as absolute velocities. However, uncertainties in the calculated ship speed due to the noise in the GPS made it difficult to extract absolute water velocities with needed confidence in May 1994 data. Thus, all offshore velocities presented for May 1994 are relative to the currents at 300 m level. Further data processing procedures used for ADCP data included error control, median filtration and statistical analysis for each level. The maps of distribution of horizontal current vectors as well as the fields of dynamic topography relative to 500 db reference level were produced. ADCP derived current vectors at 10 m level (nearest to sea surface valid ADCP data) are analyzed together with satellite thermal images.

### 2.2. SATELLITE DATA

NOAA AVHRR satellite data were obtained in HRPT mode at the MHI receiving station. Software developed in MHI was used for the pre-processing, geographical positioning and geometrical transformation of images to required projection. In the second stage of processing, radiation temperature was computed for the infrared channel 4 with a spatial resolution of 1' in the meridional direction and 1.5' in zonal direction, and a resolution of 0.1°C. Finally, the coasts, shelf boundaries and the ADCP-measured current vectors were superimposed on the images.

## 3. ADCP-measured Currents and Geostrophic Circulation.

The 10 db dynamic topography and the superposed ADCP current vectors at 10 m (Figure 1,a) of April 1993 experiment shows the main large-scale and meso-scale features described earlier, such as the meandering jet of the Rim Current, a series of quasi-stationary anticyclonic eddies on its right hand side and the cyclonic circulation pattern in the central part. Large-scale structures with maximum velocities coinciding with the RC jet west off Crimean peninsula and along the Turkish coast were well distinguished. Weaker flows are observed along the north-west shelf (10-15 cm/s), and in the central regions (20-25 cm/s) of the sea. The ADCP data reflect a more complex meso-scale current structure compared to that revealed by the CTD based geostrophic calculations. This makes them more preferable for comparison with high resolution satellite thermal images, especially in areas where higher degree of spatial variability is evident (RC meanders and frontal regions of eddies).

The main differences of geostrophic circulation in May 1994 and April 1993 are the less intensive flows of the Rim Current and the more pronounced meandering in the south (Figure 1,b). The two anticyclonic eddies to the right side of the main jet along the shelf break of the north-western shelf west of Crimea are similar in 1993 and 1994, but they are further separated in 1994 by the cyclonic meander between them. Another large quasi-stationary anticyclonic eddy in the western part of region (the so called Bulgarian eddy) has been described earlier [5]. ADCP vectors distribution almost fully reflects the details of circulation patterns in the areas where the data coincide with the hydrographic stations grid.

The comparison of current vector distributions at 6-20 m levels allowed to infer the vertical homogeneity of upper layer circulation and thus it is a good base for the interpretation of sea surface satellite imagery. Some statistical parameters of ADCP currents at 10 m depth are presented in Table 1. It is evident that much more intensive flows took place in April 1993 in comparison with May 1994. For both surveys, the average and maximum values of the zonal component  $u$  (positive eastward) were larger than meridional component  $v$  (positive northward), while the opposite was observed in the minimum current components.

It is interesting to reveal the relationship of ADCP-measured currents with the CTD-derived geostrophic flows and to determine how closely they agree with each other. A qualitative comparison of the current vector field with the dynamic topography is made and the correlation between ADCP-measured and geostrophic velocities at number of characteristic levels are examined to address these questions. Table 2 displays the correlation coefficients obtained for 10m (roughly coinciding with the upper mixed layer), 30 m (near the seasonal thermocline and the upper boundary of cold intermediate layer-CIL), 60 m (at the core of the CIL) and 100 m (below CIL and at about the depth of the main pycnocline). Better correlation was observed in 1993 compared to 1994.



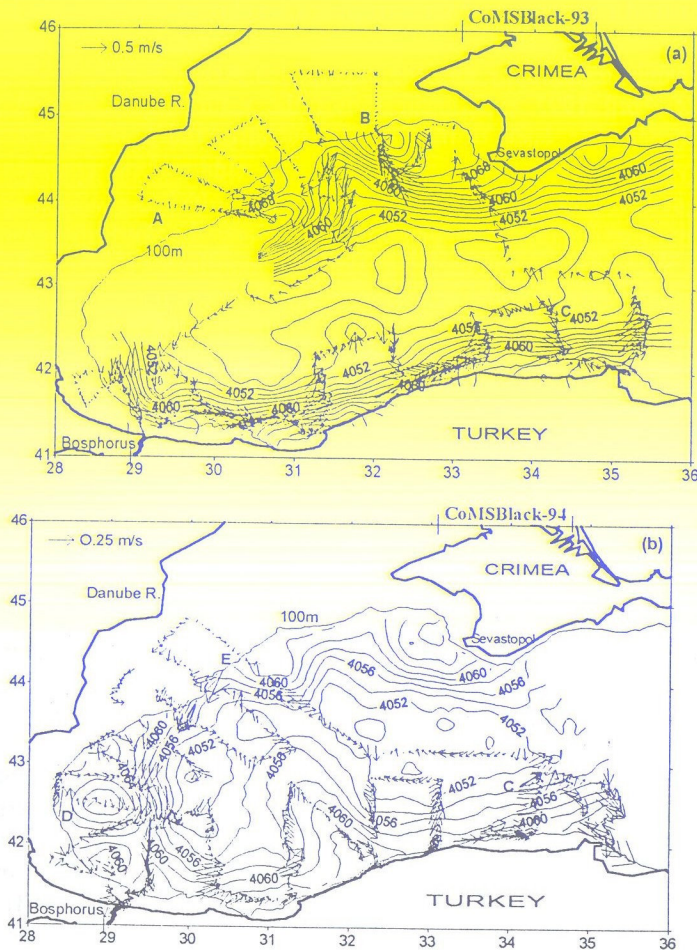


Figure 1. Dynamic topography (10 db, dyn.cm) and ADCP current vectors on 10 m in April 1993 (a) and May 1994 (b)

The u-components are also better correlated than the v-components. Figure 2 presents dynamic topography for 30 db where the best correlation was observed between the two sets of measurements. ADCP current vectors are shown for those points including the regular stations as well as those obtained along the cruise track.

For each of the two cruises, the available potential energy (APE) obtained from the CTD-measurements and the kinetic energy (KE) is calculated from the ADCP data. Table 3 contains the basin-averaged values of energy densities for selected depths as well as integrated estimates for the 10-100 m layer, providing additional quantitative verification of differences in circulation. The more energetic circulation in 1993

compared to 1994 and the changes in the KE/APE ratio ( $>1$  in 1993 and  $<1$  in 1994) are consequences of interannual and seasonal variability.

TABLE 1. Statistics of the ADCP - Current Measurements on the 10 m depth level.

Parameter	April 1993		May 1994	
	u	v	u	v
Average	8.3	0.8	3.1	-2.3
Stand Dev.	29.0	22.1	11.4	11.3
Minimum	-63.6	-70.3	-28.8	-36.9
Maximum	95.9	74.8	56.0	30.0

TABLE 2. Correlation Coefficients Between the ADCP derived currents and Geostrophic Currents based on dynamic computations.

Depth, m	April 1993		May 1994	
	u	v	u	v
10	0.81	0.72	0.65	0.46
30	0.84	0.73	0.61	0.55
60	0.80	0.67	0.62	0.54
100	0.73	0.56	0.52	0.41

#### 4. Surface Circulation and Meso-scale Thermal Features

##### 4.1. APRIL 1993

A cloud-free AVHRR scene obtained on April 19 (Figure 3) clearly shows the meandering band of warm water corresponding to the Rim Current west of Sevastopol.

TABLE 3. Basin-Averaged Energetic Parameters

Depth, m	April 1993		May 1994	
	APE, J/m <sup>3</sup>	KE, J/m <sup>3</sup>	APE, J/m <sup>3</sup>	KE, J/m <sup>3</sup>
10	10.04	65.50	19.47	11.00
30	17.17	69.60	5.53	11.35
60	61.07	69.54	20.22	11.49
100	183.15	58.82	57.29	6.69
10-100	1841	3288	765 J/m <sup>2</sup>	540 J/m <sup>2</sup>

To the south, along 44.2° N, a cold water patch is formed possibly by flow divergence and is separated into two branches. The cold anomaly ( $-1.2^{\circ}\text{C}$ ) is observed at the 'foot' of northern branch of the cyclonic meander west of Crimea. To the west of



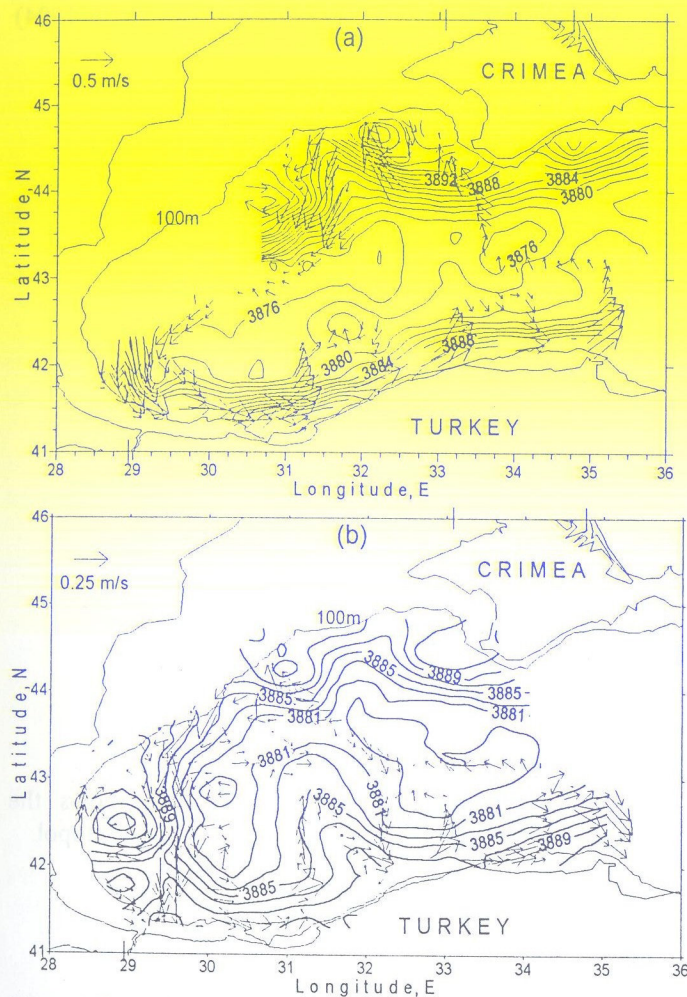


Figure 2. Dynamical topography (dyn. cm) and ADCP current vectors on 30 m depth in April 1993 (a) and May 1994 (b).

this meander, an anticyclonic eddy (Sevastopol eddy) centered at  $44.5^{\circ}\text{N}$ ,  $32.1^{\circ}\text{E}$  with a diameter of 55 km is observed (feature 1 on Fig.3). Further to the west, the cyclonic part of the meander separates the Sevastopol eddy from the next anticyclonic eddy centered at  $43.3^{\circ}\text{N}$ ,  $30.5^{\circ}\text{E}$ . It is believed that this is the same feature as an anticyclone observed during previous summer (centered at  $43.3^{\circ}\text{N}$ ,  $29.8^{\circ}\text{E}$ ), shifted west from its former position [3].

The north-west shelf is colder ( $1.5\text{--}2.0^{\circ}\text{C}$ ) than water at the shelf break. Near the western shore, the clearly traced Danube waters are warmer than the shelf water by

about  $1.5^{\circ}\text{C}$ . River waters enter to the sea through the clearly distinguished three outlets of the Danube delta and spread as a narrow band along the coast south to contribute to the off-shore anticyclonic eddy south of Cape St. George. A band of cold water originating from the northern shelf flows in between the near-shore jet and the Rim Current along the shelf.

Along the southern coast, the RC jet is distinguished by its warmer waters. An anticyclonic eddy located to the north of this jet (centered at  $42.5^{\circ}\text{N}$ ,  $31.7^{\circ}\text{E}$ ) with a cold core trapped from the surroundings appears as an anticyclonic filament shed from the rim current, with a diameter of  $\sim 40$  km and temperature gradient of about  $6^{\circ}\text{C}$  between its center and periphery (feature 2, Fig.3). A cold frontal structure starting from the Bosphorus Canyon is connected to the offshore cold water originating from the north-west shelf through a meandering band of cold water on the offshore side of the warm Danubian water (feature 3, Fig.3). Warmer water along the Turkish coast not yet effected by the cold water from the north-west is also advected by the Rim Current. Another cold region along the eastern part of Turkish coast is clearly seen in the image.

In the later satellite image of April 27, 1993, the Rim Current in the south west is not observed as continuous jet, but rather as a system containing 5-6 eddies moving east. Reformation of the flow as seen here appears to be typical of the spring-summer season in the Black Sea [6,7].

ADCP derived current vectors and the satellite thermal patterns (Figure 3) are in good correspondence in April 19, 1993. The velocity maxima in ADCP currents coincide with the temperature gradients related to the Rim Current revealed from the satellite image. The directions of the currents correspond to flow patterns derived from satellite with the stream function derived from hydrographic data (see Figures 1,a and 2,a). Moreover, the usage of satellite data assists in the interpretation of ADCP current data by meso-scale dynamic features. The following examples (some of them enlarged in Figure 4 can be pointed out:

The thermal patterns showing meanders and eddies west of Crimea allow to fill in the gaps between ship tracks in the ADCP measurements.

To the north of the Bosphorus, along  $42.0 - 42.2^{\circ}\text{N}$ , convergence in the current vectors is observed. Based on the satellite image, the reason for this phenomenon is inferred to be the confluence of southward flowing warm jet along  $29.4^{\circ}\text{E}$  and the cold water tongue directed south-east (Fig.4,a).

The northward directed current vectors along the western shelf in the middle part of the ship track between  $31.3$  and  $32.3^{\circ}\text{E}$ , at about  $42.4^{\circ}\text{N}$ , and the south-westward currents in the northern part of next north-south ship track can only be understood in reference to satellite data showing a small but coherent anticyclonic eddy through which the ship track happened to pass across its south-west periphery (Fig.4,b).



## 4.2. MAY 1994

The NOAA AVHRR thermal image received on 5 May, 1994 demonstrates good agreement with geostrophic flow and ADCP vectors in the cloud-free north-western and east-western parts of the scene (Figure 5). The main meso-scale thermal features explained by dynamical features are the following. The eastern (centered at  $44.6^{\circ}\text{N}$ ,  $32.5^{\circ}\text{E}$ ) and western cores of the Sevastopol anticyclonic eddy to the west of Crimea (features 1,2, Fig.5). The last one is crossed by ADCP vectors on its southern and south-western edges.

The Bulgarian anticyclonic eddy centered at  $42.5^{\circ}\text{N}$ ,  $29.0^{\circ}\text{E}$  about 80 km width is fully described by all available observations (feature 4 on Fig.5). To its north, a small anticyclonic eddy at Cape Kaliakra (feature 3, Fig.5) is observed.

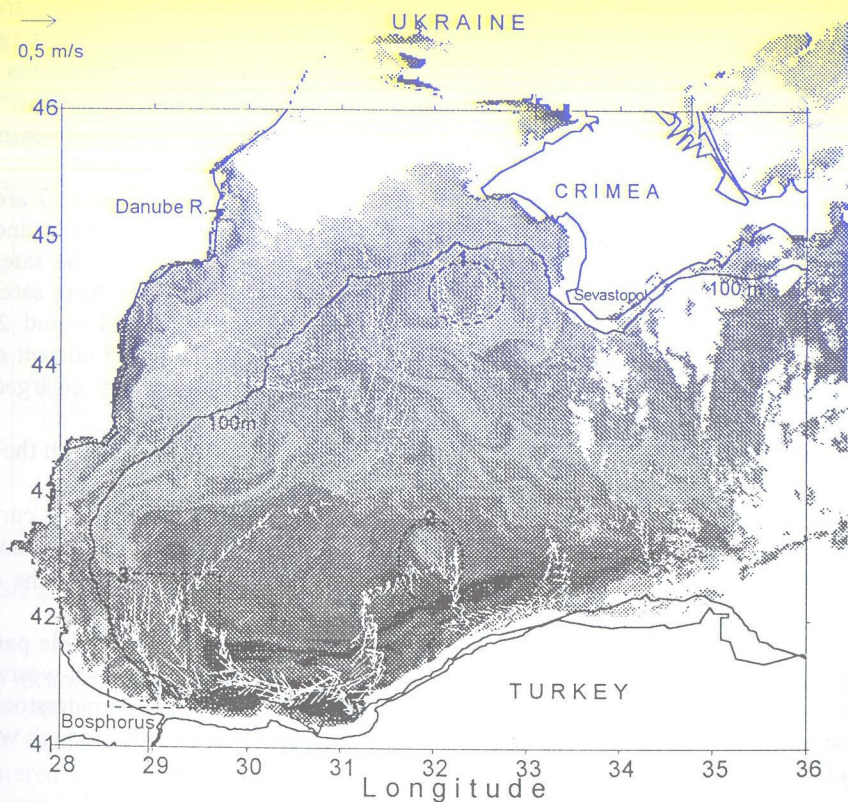


Figure 3. NOAA AVHRR thermal image for April 19, 1993. Dark tones correspond to warm water. Shoreline and shelf edge (black solid line). ADCP current vectors (white arrows) for 10 m depth are superimposed and main meso-scale features are contoured (black dash line)

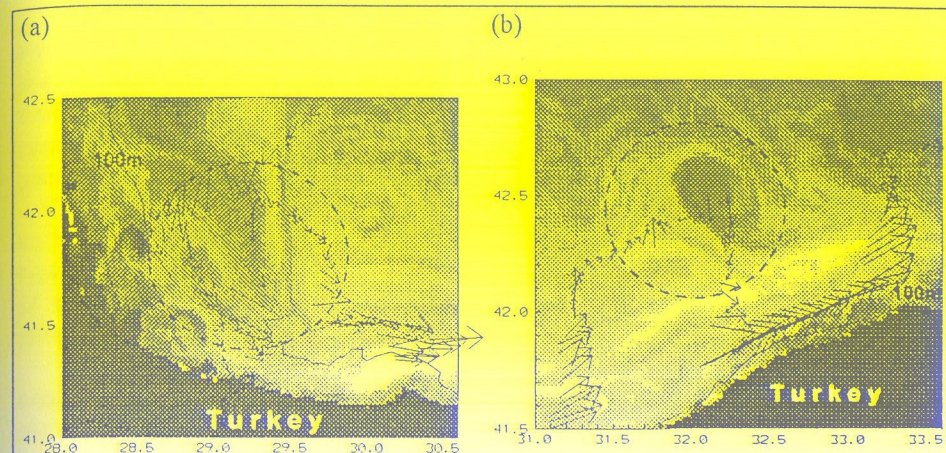


Figure 4. Fragments of NOAA AVHRR Channel 4 image for 19 April, 1993 with the ADCP current vectors superimposed. Darker tones correspond to cooler water while lighter ones - to warmer sea surface water. Land and clouds are masked by black color. Dash-line circles indicate the meso-scale features discussed in text.

In the Bosphorus region, the convergence of the RC and the along shore stream on the shelf appears to replicate the features observed in previous year (feature 4, Fig.5).

A large anticyclonic eddy-meander system on the southern branch of the Rim Current with a cross-meander scale of  $\sim 160$  km and a wavelength of 140 km (feature 5, Fig.5). These features are typical of the meander and eddy generation by Rim Current jet instability consistently observed along the same coast [2,4,7].

## 5. Discussion and Conclusions.

It should be noted that close correspondence between the measured current parameters and thermal circulation structures in the cases considered has obviously seasonal character since the conditions during the cruises were preceding to seasonal thermocline development. Later on, the reformation of temperature field took place as it was seen from the latest satellite images. It remains uncertain whether these changes will reflect a close relation between meso-scale temperature and current fields peculiarities in summer season. This question requires further experimental investigations. But comparing the results obtained at this moment, we can expect much worth agreement between the currents and temperature fields because of total weakening of the RC jet flows and seasonal heating of the sea upper layer (that masks the influence of the water circulation on the sea surface).



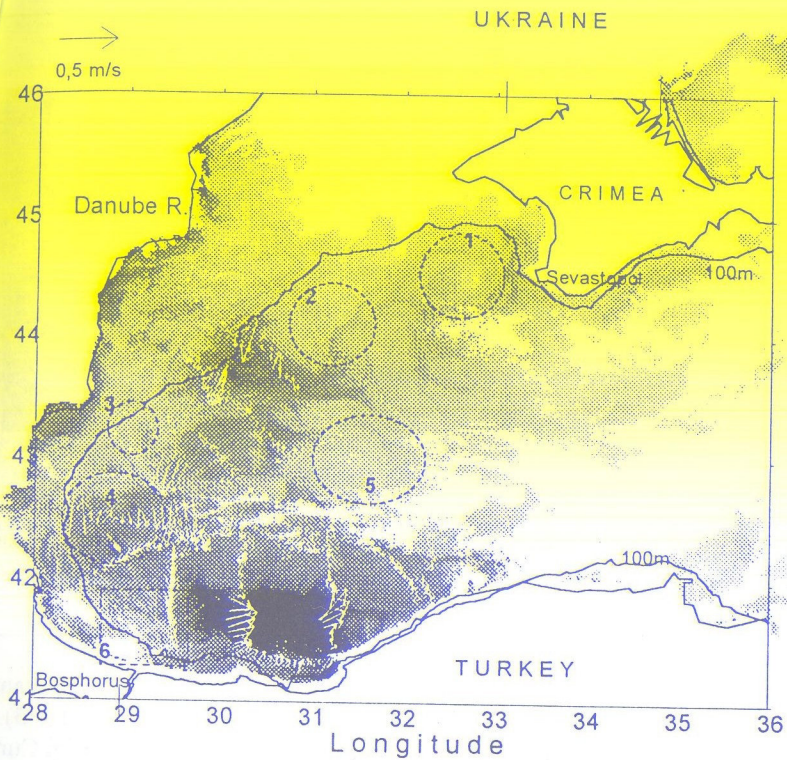


Figure 5. NOAA AVHRR thermal image for May 5, 1994. Dark tones correspond to warm water. Shoreline and shelf edge (black solid line), ADCP current vectors (white arrows) for 10 m depth are superimposed and main meso-scale features are contoured (black dash line)

The April 1993 data were obtained just before the circulation reconstruction from the winter type to summer one. That is why the average and maximal current speed are about twice higher than for the May 1994 observations (see Table 1). During the CoMSBlack-94 survey, such reconstruction had probably started. The evidences are less intensive stream flows as well as the more pronounced meandering of the Rim Current. The comparison of correlation coefficients (see Table 2) gives us an additional reason to conclude that May 1994 data were sampled during the total circulation reconstruction. Geostrophic currents are determined by total baroclinic layer stratification and they are more conservative (geostrophic adjustment period for the Black Sea is about 1 month), while ADCP-measured currents are quasi-instant and reflect both time and spatial changes during the survey period (20 days). So, smaller correlation between them can be due to delay in reconstruction of geostrophic circulation pattern from the real currents changes.

As the main conclusion, it can be noted that the ADCP current vectors and thermal structures at the sea surface displayed very good agreement. The velocity maxima coincide with the temperature gradient location within the Rim Current and vector directions correspond to satellite derived flow configuration. Satellite data assist essentially in the interpretation of ADCP data by way of explaining some specific peculiarities in vector distribution as a manifestation of meso-scale dynamic features.

To describe the details of the structure of currents and cross-isobaths water exchange, the vertical section of horizontal current components were produced for typical dynamical situations (eddies at the shelf-break and RC jet flows). The peculiarities of the cross-isobaths component of movement supplement the patterns of dynamic phenomena obtained by along-isobath velocity distributions.

The volume transport in normal direction to the ADCP transects were evaluated. To understand how to distinguish the transport in the meandering jet from the transport within the eddies it has been compared for the well-recognized in dynamical topography anticyclonic eddies at the shelf break, RC jet and for the both types of dynamics sampled together.

Presented results of integrated data analyses allow to provide additional oceanographic background for the numerical modelling of the Black Sea general and meso-scale circulation as the basis for an ecosystem monitoring.

**6. Acknowledgments.** This study was supported by the NATO TU-Black Sea Project. The R/V Bilim measurements were supported by Scientific and Technical Council of Turkey.

## 7. References

- Oguz T., La Violette P.E. and Unluata U. (1992) The Upper Layer Circulation of the Black Sea: Its Variability as Inferred from Hydrographic and Satellite Observations, *J. of the Geophys. Res.*, **97**, 12569-12584.
- Oguz T., Latif V.S., Latif M.A., Vladimirov V. L., Sur H.I., Markov A.A., Ozsoy E., Kotovshchikov B.B., Eremceev V.N. and Unluata U. (1993) Circulation in the Surface and Intermediate Layers of the Black Sea, *Deep-Sea Research*, **41** (8), 1597-1612.
- Ilyin Y.P. (1995) Anticyclonic Eddies Near the Continental Slope Edge of the North-Western Black Sea: the Formation of Surface Imagery and Satellite IR Observations in Spring-Summer Time", In V.N. Eremceev (Chief Ed.) et al., *Investigations of the Shelf Zone of the Azov-Black Sea Basin*, MHI UNAS, Sevastopol, pp. 22-30.
- Sur, E. Ozsoy, Y.P. Ilyin and U. Unluata (1996) Coastal/Deep Ocean Interactions in the Black Sea and their Ecological/Environmental Impacts", *Journal of Marine Systems*, **7**, 293-320.
- Oguz, T., S. T. Besiktepe, L. Ivanov, V.Diaconu (1998) On the ADCP derived Rim Current structure, CIW formation and the role of mesoscale eddies on the CIW transport in the Black Sea. (this issue).
- Stanev E., Truhchev D.I. and Roussenov V.M. (1988) The Black Sea Water Circulation and Numerical Modelling of Currents, Sofia University. Sofia.
- Golubev Y.N. and Tuzhilkin V.S. (1990) Some Aspects of the Synoptic Variability of the Black Sea Hydrophysical Fields, MHI UNAS, Sevastopol.